Academia and Society
International Journal of Education and Society

HOLY CROSS

Print ISSN : 2393-9419
Online ISSN : 2393-8919

AAS 2025: 12 (1)

Biosoftening of Lignin in Sugarcane Bagasse Using Pleurotus Sajor-Caju: A Sustainable Approach for Enhancanced Reactivity in Resin- Production

Sowmya Kuppusamy
Assistant Professor
PG and Research Department of Biotechnology & Bioinformatics
Holy Cross College, Trichy, TamilNadu. India

ABSTRACT

This study investigates the biosoftening of lignin in sugarcane bagasse using the white-rot fungus Pleurotus sajor-caju through solid-substrate fermentation. Bagasse, a ligno cellulosic waste rich in lignin (21%), was inoculated with fungal spawns and incubated for five weeks. Lignin was extracted weekly via alkaline delignification and analyzed using UV spectroscopy and FT-IR to assess structural changes. Results showed a progressive decline in lignin yield—from 62.2% at week 0 to 15.38% by week 5—indicating effective fungal degradation. UV scans revealed reduced absorbance at 260–280 nm and shifts in λ max, suggesting cleavage of aromatic rings and demethoxylation. FT-IR analysis confirmed the breakdown of key lignin structures, including aromatic skeletal vibrations (1600–1510 cm^{-1}), O–H stretching (~3420 cm^{-1}), and ether linkages (1120–1030 cm^{-1}), alongside the emergence of carbonyl groups (~1720 cm^{-1}), signaling oxidative depolymerization. These modifications enhance lignin's reactivity, making it more suitable for resin synthesis, particularly lignin–phenol–formaldehyde (LPF) resins. The study demonstrates that P. sajor-caju offers an eco-friendly, cost-effective alternative to chemical softening methods, reducing environmental impact while valorizing agricultural waste. The findings support the use of white-rot fungi in sustainable bioprocesses for industrial lignin modification and the production of bio-based polymers.

Keywords: Lignin, Biosoftening, Pleurotus Sajor-Caju, Solid-Substrate Fermentation, Sugarcane Bagasse, Ligninolytic Enzymes, FT-IR Analysis, UV Spectroscopy

Received: 17 June 2025, Revised 10 August 2025, Accepted 17 August 2025

DOI: https://doi.org/10.6025/aas/2025/12/1/1-20

1. Introduction

India ranks second in sugarcane production, behind Brazil. The spent fibres after sugar extraction from sugarcane are bagasse. Bagasse is a lignocellulosic agricultural waste and a source of lignin. The dry bagasse consists of 39% cellulose, 37% hemicellulose, 21% lignin, and 3% ash (Yogitha et al., 2020). It is used to make pulps, board materials, and composites (Wongsangprai C., 2012). Agro industrial wastes are produced in large quantities worldwide and pose environmental and human health risks (M. N. Shashirekha, 2002).

Mushrooms are among the fastest growing fungi and are rich in nutrients. They are included in diets globally. The consumption rate of mushrooms has increased due to their nutritive value (Nelliyat, P., 2023). They are a good source of vitamins, minerals, dietary fibre and serve as a good alternative to meat. They also have higher levels of amino acids, such as glutamic acid, aspartic acid, alanine, and arginine (Oei P. (2003)). It also exhibits anti-inflammatory and immunostimulatory properties (Caglarirmak N 2007). One of the characteristic features of oyster mushrooms is that they grow well on agricultural wastes. They are found growing in layers one upon the other (Kurt S, Buyukalaca S., 2010).

Pleurotus sajor caju is a mushroom which has high nutritional and therapeutic value. It is also reported to possess anti-inflammatory, antitumour, anti hypertensive, and antioxidant properties (Wasser, S.P., 2002). Pleurotus sajor caju produces lignolytic enzymes, including manganese peroxidases, lignin peroxixidases, phenol oxidases, and laccases. Fungi have applications in the environmental and biotech sectors (Wan Rosli, 2012). The enzymes secreted by fungi into the extracellular medium have potential roles in delignifying cellulose pulp, pulp discolouration, coal processing, and oil refining (Barreira *et al.*, 2014). The fungi, when used in an experiment in the paper mill effluent treatment, were found to reduce the total polyphenols and the colour present in the effluent (Mane V.P *et al.*, 2007).

2. Related Research

Date palm leaves are rich in minerals, cellulose, and lignin, and thus serve as a substrate for the production of oyster mushrooms. In recent years, polymers have been developed from renewable resources due to increased environmental pollution and declining fossil feed stocks. Some biobased polymers synthesised from renewable biomass include polyesters, epoxy resins, polyurethanes, and cyanate esters. So, developing high performance polymers from renewable resources offers an alternative to petroleum based polymers. Lignin is a biobased polymer derived from wood. Recent developments have led to the use of lignin and its derivatives as additives in agriculture and building materials (Meiyu Huo *et al.*, 2024). They also find its application as a water pollution treatment agent and a petroleum extraction active agent. Resin preparation using lignin has received much attention, as it exhibits excellent thermal and thermo-oxidative stability, a high glass transition temperature, and outstanding flame resistance. In particular, the new lignin derived phthalonitrile resin is used in aerospace, submarine, and microelectronics applications (Asada C et al., 2014).

Pleurotus sajor-caju effectively biosynthesises lignin through enzymatic depolymerisation, reducing lignin's molecular weight and transforming ligno cellu-

losic materials. There is increasing interest in developing enzyme-assisted bioremediation processes due to their low energy requirements, mild operational conditions, and potential to reduce the formation of harmful by pro- ducts. (Helena Sá, 2024, C. Ji, 2016)

Multiple studies demonstrate its lignin degrading capabilities: D. S. Chahal et al. showed the fungus depolymerises lignin into progressively smaller oligolignol molecules, with evidence of both breakdown and potential repolymerization. The lignolytic edible fungi, of which Pleurotus sajor-caju is one, are efficient agents for valorising vegetable wastes that cause environmental pollution, in the context of food production and the struggle against malnutrition and food insecurity (Mpadi, N. C., & Bangala, D.-B.). M. (2020).

Our work aimed to use the lignin material as a base for resins. So, it is necessary to soften the lignin for resin preparation. Because chemical softeners are harmful and costly for large-scale production, we opt for biosoftening using *Pleurotus sajor-caju*. Solid-substrate fermentation was performed using Bagasse as the substrate and Pleurotus sajor-caju as the inoculum. Extracted lignin was analysed by UV scanning and FT-IR to assess structural changes. They can be exploited commercially for the preparation of resins.

3. Materials and Methods

3.1 Collection of Bagasse Sample

The crushed bagasse was collected from a sugar factory situated near Karur. The collected sample was dried in a hot-air oven at 80 °C overnight to reduce its moisture content to 25-30%.

Figure 1. Bagasse Collected from Sugar Mill

Figure 2. Pleurotus sajor-caju Spawns

Crushed sugarcane bagasse obtained from the Karur sugar factory, before drying. The material initially contained ~50% moisture.

3.2 Collection of Mushroom Spawns. (*Pleurotus sajor-caju*)

Commercial mushroom spawns procured from the Tamil Nadu Agricultural University (TNAU), Virinjipuram, were used as inoculum for solid-substrate fermentation.

3.3 Packing Of Bagasse With Mushroom Spawns (*Pleurotus Sajor-caju*)

Bagasse was sprinkled with water before packing. Twelve polythene bags measuring 19×15 cm were used, and holes were evenly punched for aeration. Of these, six bags were filled solely with bagasse, serving as control samples. The other six bags were filled with bagasse and mushroom spawn and served as test samples. The inoculum taken was 10%. These bags were incubated for 5 weeks in a moist chamber with intermittent sampling.

Polythene bags containing bagasse (control) and bagasse inoculated with *P. sajor-caju* (treatment), prepared for incubation in a moist chamber.

Figure 3. Packed Control and Treated Fermentation Bags

Figure 4. Polythene bags containing bagasse (control) and bagasse inoculated with *P. sajor-caju* (treatment), prepared for incubation in a moist chamber

3.4 Sampling

The zeroth week sample was collected immediately after packing. The samples were collected at the end of each week and labelled as first week, second week, third week, fourth week, and fifth week, respectively.

Figure 5. Fungal-Treated Bagasse Samples

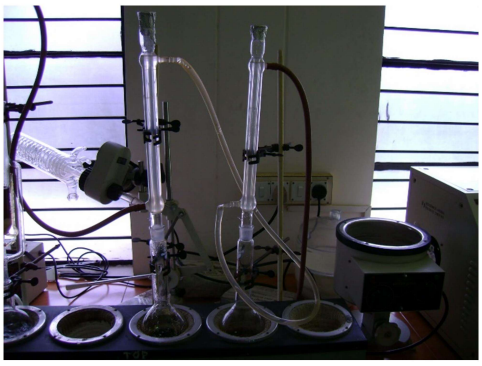

Figure 6. Alkaline Delignification Setup

Changes in the visual appearance and texture of bagasse after colonisation by *P. sajor-caju* over multiple weeks.

3.5 Extraction of Lignin

Delignification was performed in a round-bottomed flask, fitted with a condenser. Bagasse (5 g) and 5 M sodium hydroxide (100ml) were charged to a flask. The temperature was maintained at 100 ± 1°C for seven *h*. The black liquor obtained was filtered through glass wool to remove suspended pulp fibres, then neutralised with 50% H2SO4 solution under constant stirring. The precipitated lignin was centrifuged at 8000rpm for 10 minutes, and the pellet was washed repeatedly with hot distilled water until a constant weight was obtained. A lignin cake was obtained, dried overnight at 60°C, and used for further analysis. This Delignification was performed on all biologically treated samples, as well as on dry bagasse (5 g) that was not treated with mushrooms.

Round-bottom flask fitted with a condenser used for lignin extraction under alkaline conditions (5 M NaOH, 100 °C).

Figure 7. Black Liquor After Alkaline Extraction

Figure 8. Neutralization of Black Liquor

Alkaline-solubilized lignin (“black liquor”) obtained after 7 h delignification.

Precipitation of lignin following acidification of black liquor with 50% H, SO, under constant stirring.

Figure 9. Lignin Precipitate Formation

Figure 10. Dried Lignin Cake

Insoluble lignin fraction obtained after acid neutralization and separation.

Dried lignin cake after repeated washing and oven drying at 60 °C.

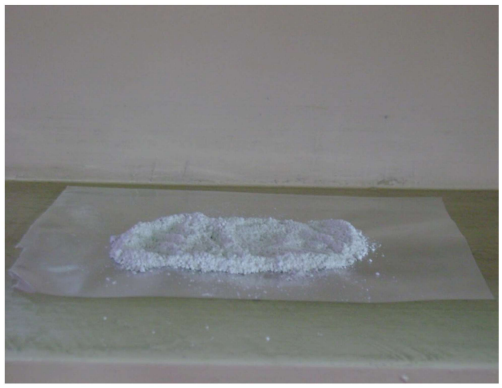

Figure 11. Lignin Extracted from Treated Samples

Figure 12. Lignin Extracted from Untreated Bagasse

Purified lignin obtained from *P. sajor-caju*–treated bagasse showing reduced yield and altered color.

Lignin extracted from the control (uninoculated) bagasse showed a comparatively higher yield.

Figure 13. Commercial Lignin

Reference lignin purchased for comparative spectral analysis.

3.6 Lignin Analysis

The lignin samples (treated, control, and commercial) were subjected to Ultraviolet (UV) scanning and Fourier Transform Infrared (FTIR) analysis.

3.6.1 Uv Scanning

The lignin samples were dissolved in dioxane at a concentration of 1mg/ml. UV scanning was performed over the 200-400 nm range. Commercial lignin was also disbanded at the same concentration and scanned over the same wavelength range, yielding the same peaks. The instrument used for UV Scanning is a HITACHI U-2800 Spectrophotometer.

3.6.2 FT-IR:

The lignin sample was mixed with Potassium Bromide (KBr) at a 1:50 ratio. The mixture was then analysed using an Avatar 330 FT-IR (Thermo Nicolet).

4. Results and Discussion

4.1 Percentage Yield of Lignin

Sampling Week	Dry Weight of Substrate (g)	Dry Weight of Extracted Lignin (g)	Lignin Yield (%)
0 (Baseline)	5.00	3.11	62.20
1	5.00	2.588	51.76
2	5.00	1.696	33.92
3	5.00	1.351	27.02
4	5.00	1.242	24.84
5	5.00	0.769	15.38

Table 1. A steady reduction in lignin yield was observed across the 5-week fermentation period, indicating progressive lignin degradation by *Pleurotus sajor-caju*

Table 1 indicates that lignin yield was lower in subsequent weeks. This shows that the lignin has been degraded by the fungus *pleurotus sajor caju* during solid substrate fermentation. The lignin percentage in the 5th week of the treated samples reveals this.

Before biosoftening, the lignin content was higher. Table 1's reduction in the treated sample lignin content made it abundantly evident that the *P. sajor caju* fungus increased the lignin reduction. The lignin content decreased from 62.2% after 1 week to 51.76% at the end of the 3rd week, a 27% decrease. After 4 weeks, it was found to be a weak lignin degrader, with lignin yield decreasing from 27.02% to 24.84%. By the end of the 5th week, the lignin content had been reduced to 15.38%.

The lignin yield from bagasse during solid-substrate fermentation with *Pleurotus sajor-caju* is presented in Table 1. A steady reduction in lignin content was observed across the five-week period. Initially, at week 0, the yield was 62.2%; it decreased to 51.76% after the first week and further declined to 15.38% by the fifth week.

This progressive reduction clearly indicates that *P. sajor-caju* effectively degrades lignin. The significant loss of lignin content after the third week suggests increased enzymatic activity of lignin-degrading enzymes, including lignin peroxidase, man-

ganese peroxidase, and laccase. Similar reports of lignin degradation by *Pleurotus* species have been made in agro-residue treatments, where a reduction in lignin content enhanced substrate digestibility and facilitated further utilisation for industrial applications.

Although the decline was rapid during the first three weeks, the rate of reduction slowed during the fourth and fifth weeks, indicating a saturation phase in fungal metabolism or depletion of easily degradable lignin fractions. This observation is consistent with other studies showing that white-rot fungi initially degrade accessible phenolic structures before acting on more complex condensed lignin moieties.

4.2 Uv Scanning

UV scanning of the treated lignin samples revealed distinct spectral changes compared to untreated and commercial lignin. The untreated lignin exhibited strong absorbance at 280 nm, characteristic of aromatic rings with conjugated double bonds. In contrast, treated samples showed shifts in ëmax and reduced absorbance intensities over successive weeks.

These spectral shifts indicate structural modifications such as cleavage of aromatic rings, demethoxylation, and breakdown of chromophoric groups. The decrease in absorbance in the 260–280 nm region further supports lignin depolymerisation. Notably, the appearance of multiple peaks in some treated samples suggests the formation of intermediate low-molecular-weight aromatic compounds.

The UV results therefore confirm partial breakdown of lignin macromolecules by fungal action, consistent with the declining lignin-yield data.

The present study demonstrates the effectiveness of *Pleurotus sajor-caju* in degrading and softening lignin in sugarcane bagasse via solid-substrate fermentation. Visual observations of fungal colonisation (Figures 3–5) confirmed successful substrate utilisation during the incubation period, which corresponded closely with the progressive reduction in lignin yield (Table 1). The steady decline from 62.20% (week 0) to 15.38% (week 5) clearly indicates significant ligninolytic activity, consistent with the known enzymatic capabilities of white-rot fungi.

The observed degradation trend suggests that *P. sajor-caju* preferentially targets readily accessible phenolic units during the early weeks, resulting in a sharp decline in lignin content by week 3. The slower degradation observed in weeks 4–5 aligns with the depletion of low-molecular-weight and less-cross linked fractions, leaving more recalcitrant components that degrade at a reduced rate. This pattern is typical of white-rot fungal systems, where enzymes such as laccases, manganese peroxidase, and lignin peroxidase progressively depolymerize lignin via oxidative mechanisms.

The UV–visible spectral data provide important insights into the structural modifications occurring in lignin during biosoftening by *Pleurotus sajor-caju*. Lignin typically exhibits strong absorption in the 260–280 nm region due to its aromatic

rings and conjugated phenolic structures. Changes in λmax values and absorbance intensities, therefore, reveal alterations to chromophoric groups wit- hin the lignin polymer.

Sample	Peak Type	Start (nm)	Apex (λmax, nm)	End (nm)	Absorbance
Commercial Lignin	Primary	400.0	383.0	200.0	10.000
Week 1 (Treated)	Primary	400.0	267.0	255.5	0.086
Week 2 (Treated)	Primary	400.0	262.5	255.0	0.214
Week 3 (Treated)	Primary	400.0	262.5	259.5	0.229
Week 3 (Treated)	Secondary	259.5	247.5	200.0	10.000
Week 4 (Treated)	Primary	400.0	343.0	335.0	0.017
Week 4 (Treated)	Secondary	335.0	262.5	255.0	0.159
Week 5 (Treated)	Primary	400.0	262.5	257.0	0.251
Week 5 (Treated)	Secondary	257.0	247.5	200.0	10.000
Untreated Lignin (Control)	Primary	400.0	261.0	255.0	0.108

Table 2. (Cleaned). UV–Visible Characteristics of Lignin Samples Classified by Week

The UV–visible spectral data provide important insights into the structural modifications occurring in lignin during biosoftening by *Pleurotus sajor-caju*. Lignin typically exhibits strong absorption in the 260–280 nm region due to its aromatic rings and conjugated phenolic structures. Changes in λmax values and absorbance intensities, therefore, reveal alterations to chromophoric groups within the lignin polymer.

4.3 Commercial and Untreated Lignin

The commercial lignin displays a very high absorbance (10.000) with a λ*max* at 383 nm, reflecting its highly condensed aromatic structure and the presence of intact conjugated moieties.

The untreated bagasse lignin shows a λ*max* at 261 nm with moderate absorbance (0.108), characteristic of native lignin containing guaiacyl and syringyl phenolic units. Together, these serve as benchmarks representing fully intact aromatic net- works.

Wave number (cm{ ¹)	Functional Group	Interpretation	Observations in Treated Samples
~3420	O–H (phenolic/ alcoholic)	stretching Hydrogen -bnonded groups	hydroxyl Intensity decreased → demethoxylation
~2920	C–H (CH, /CH*f*)	stretching Aliphatic chains	Reduced intensity indicates side-chain oxidation
1600–1510	Aromatic vibrations	skeletal Aromatic ring structures	Significant decline → aromatic ring cleavage
~1720	C=O stretching	Aldehydes/ ketones/ carboxyls	A new band appeared in the treated samples
1120–1030	C–O stretching	Alcohol/ ether linkages	Lower intensity → ether bond cleavage

Table 3. Summary of FT-IR Functional Group Assignments

The FT-IR analysis provides detailed insight into the structural transformations occurring in lignin during biosoftening by *Pleurotus sajor-caju*. Each functional group listed in Table 3 corresponds to key lignin bonds typically associated with phenolic units, aromatic rings, aliphatic side chains, or ether linkages. Comparison of treated and untreated samples reveals the nature and extent of fungal degradation.

The FT-IR results collectively demonstrate that *Pleurotus sajor-caju* causes substantial chemical and structural alteration of lignin, including: Aromatic ring disruption, Demethoxylation and oxidative conversion of phenolic components, Cleavage of ether bonds (β-O-4 linkages) and side chains, and Formation of oxidised, low-molecular-weight products. These changes are entirely consistent with white-rot fungal ligninolysis and clearly support the conclusion that the fungus biosoftens lignin by oxidative depolymerization. This structural breakdown enhances lignin's reactivity and suitability for applications such as lignin–phenol–formaldehyde resin synthesis, confirming the industrial relevance of the biosoftening process.

4.4 UV–Visible Spectral Changes and Lignin Depolymerization

UV scanning provided insight into chromophore modification within the lignin polymer. Untreated bagasse lignin and commercial lignin exhibited strong absorbance near 280 nm, reflecting characteristic aromatic structures (Figure set corre-

sponding to Table 2). Treated samples, however, exhibited reduced abs- orbance intensities, shifts in λ max, and the appearance of secondary peaks associated with intermediate aromatic compounds. These spectral changes demo- nstrate disruption of conjugated phenolic systems and oxidation of aromatic rings. The greater the fermentation duration, the more pronounced the spectral shifts—corroborating the chemical softening of lignin.

4.5 FT-IR Analysis Reveals Functional Group Modifications

FT-IR spectra offered direct evidence of structural modifications to lignin across treatments (Figures 14–16). Untreated and commercial lignin exhibited classical features of intact lignin, including strong O–H, C–H, aromatic skeletal, and C–O stretching bands. Treated samples showed: Decline in intensities of aromatic skeletal vibrations (1600–1510 cm^{-1}), indicating aromatic ring cleavage, reduced O–H stretching bands (~3420 cm^{-1}), consistent with demethoxylation loss of C–O and ether linkage bands (1120–1030 cm^{-1}), showing cleavage of β–O–4 linkages emergence of a new band near 1720 cm^{-1}, signifying formation of carbonyl-containing products such as aldehydes and carboxylic acids. These changes collectively confirm oxidative depolymerisation and increased functionalization of lignin, making it more reactive for subsequent resin synthesis.

4.6 Implications for Resin Manufacturing

The structural softening and depolymerisation observed here highlight *P. sajor-caju* as a promising biological tool for improving lignin reactivity. Softened lignin enhances crosslinking efficiency in lignin–phenol–formaldehyde (LPF) resins, reducing the need for synthetic phenols and lowering environmental impact. Compared with chemical softening techniques, biological softening reduces chemical load and processing costs, minimises ecological toxicity, and yields functionalized lignin with improved reactivity. This positions fungal biosoftening as a sustainable alternative for resin and polymer industries.

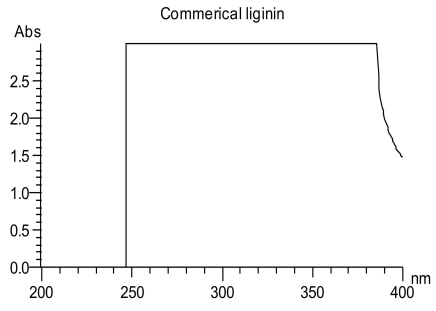

Figure 14. UV Scanning Spectrum of Commercial Lignin

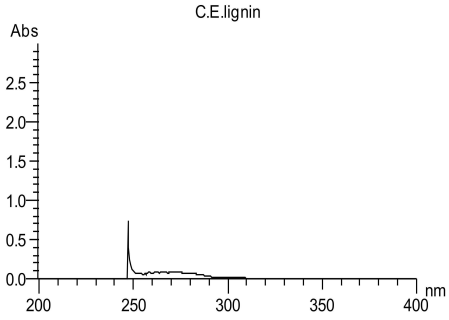

Figure 15. UV Scanning Spectrum of Untreated Bagasse Lignin

Start (nm)	Apex (nm)	End (nm)	Absorbance
400.0	383.00	200.0	10.000
Start (nm)	Apex (nm)	End (nm)	Absorbance
400.0	267.0	255.5	0.086

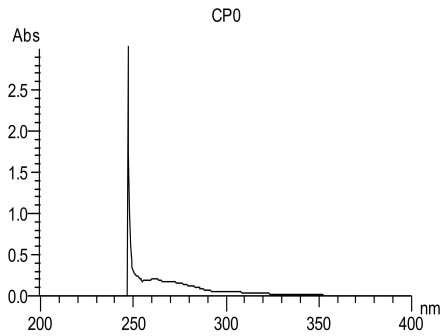

Figure 16. UV scanning Spectrum of Treated Lignin – zeroth Week (Control sample)

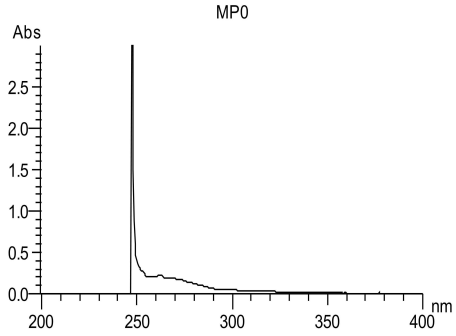

Figure 17. UV Scanning Spectrum of Treated Lignin zeroth Week

Start (nm)	Apex (nm)	End (nm)	Absorbance
400.0	262.5	255.0	0.214
Start (nm)	Apex (nm)	End (nm)	Absorbance
400.0	262.5	259.5	0.229
259.5	247.5	200.0	10.000

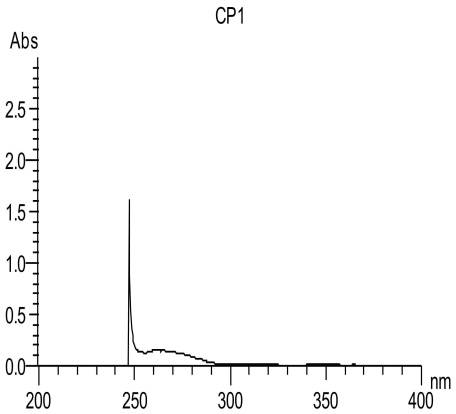

Figure 18. UV scanning Spectrum of Treated Lignin – Week 1 (Control sample)

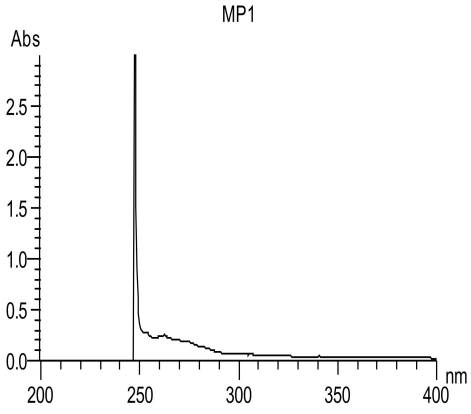

Figure 19. UV scanning Spectrum of Treated Lignin – Week 1

Start (nm)	Apex (nm)	End (nm)	Absorbance
400.0	343.0	335.0	0.017
Start (nm)	Apex (nm)	End (nm)	Absorbance
400.0	262.5	257.0	0.251

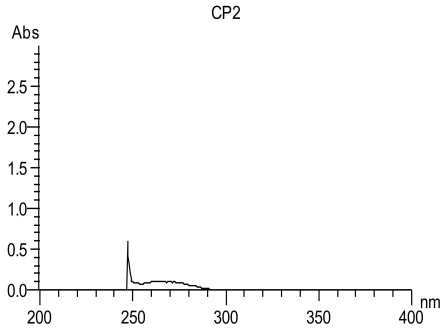

Figure 20. UV scanning Spectrum of Treated Lignin – Week 2 (Control sample)

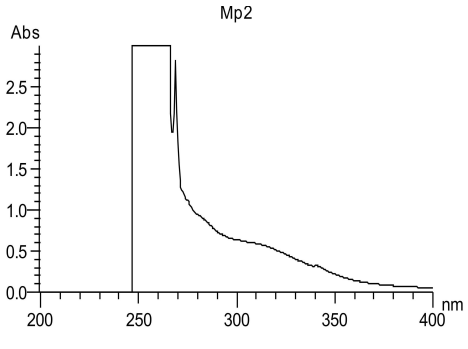

Figure 21. UV scanning Spectrum of Treated Lignin – Week 2

Start (nm)	Apex (nm)	End (nm)	Absorbance
400.0	261.0	255.0	0.108
Start (nm)	Apex (nm)	End (nm)	Absorbance
400.0	340.5	339.0	0.333
339.0	264.5	200.0	10.000

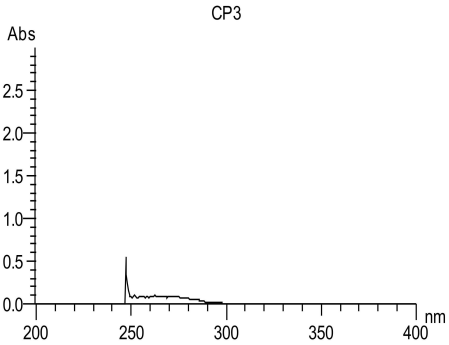

Figure 22. UV scanning Spectrum of Treated Lignin – Week 3 (Control sample)

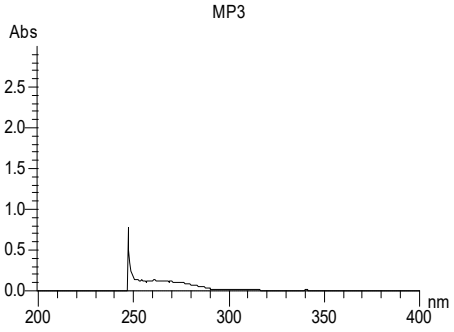

Figure 23. UV scanning Spectrum of Treated Lignin – Week 3

Start (nm)	Apex (nm)	End (nm)	Absorbance
400.0	262.5	259.5	0.099
Start (nm)	Apex (nm)	End (nm)	Absorbance
400.0	260.5	256.5	0.132

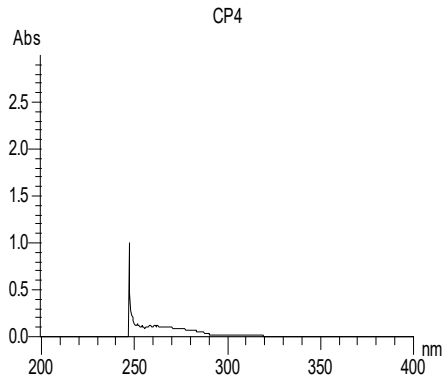

Figure 24. UV scanning Spectrum of Treated Lignin – Week 4 (Control sample)

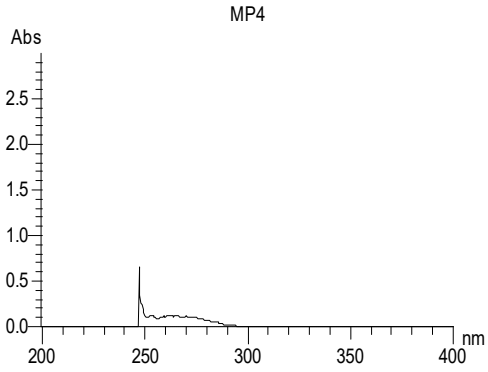

Figure 25. UV Scanning Spectrum of Treated Lignin – Week 4

Start (nm)	Apex (nm)	End (nm)	Absorbance
400.0	258.0	255.5	0.120
Start (nm)	Apex (nm)	End (nm)	Absorbance
400.0	263.0	256.5	0.125

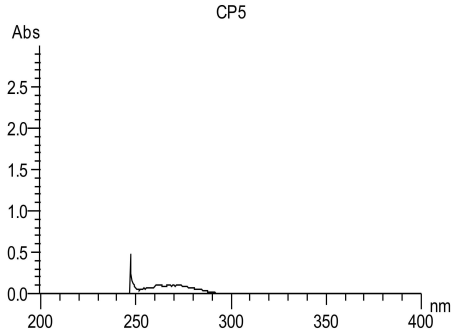

Figure 26. UV scanning Spectrum of Treated Lignin – Week 5 (Control sample)

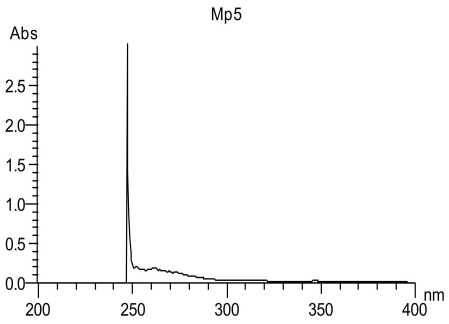

Figure 27. UV scanning Spectrum of Treated Lignin – Week 5

Start (nm)	Apex (nm)	End (nm)	Absorbance
400.0	340.5	329.5	0.008
329.5	263.0	252.0	0.107
Start (nm)	Apex (nm)	End (nm)	Absorbance
400.0	261.5	257.0	0.194

4.7 FT-IR Spectrum

FT-IR spectra provided further evidence for lignin modification. Commercial lignin displayed characteristic bands at ~3420 cm^{-1} (O–H stretching in phenolic and alcoholic groups), ~2920 cm^{-1} (C–H stretching in methyl and methylene groups), ~1600–1510 cm^{-1} (aromatic skeletal vibrations), and ~1120–1030 cm^{-1} (C–O stretching in alcohols and ethers). Untreated lignin from bagasse exhibited a similar profile, confirming the presence of intact aromatic and phenolic structures typical of lignin. Treated samples, however, showed decreased intensity in the aromatic skeletal bands (1600–1510 cm^{-1}), suggesting ring cleavage. The reduction in O–H and C–O stretching bands indicated demethoxylation and cleavage of ether linkages. Appearance of new peaks in the carbonyl region (~1720 cm^{-1}) implied oxidation of lignin side chains into aldehydes, ketones, or carboxylic groups.

These FT-IR spectral modifications demonstrate significant structural alteration of lignin after fungal treatment. The breakdown of aromatic rings and introduction of carbonyl functionalities reflect oxidative depolymerization, which is crucial fo -r softening lignin and improving its reactivity for resin production.

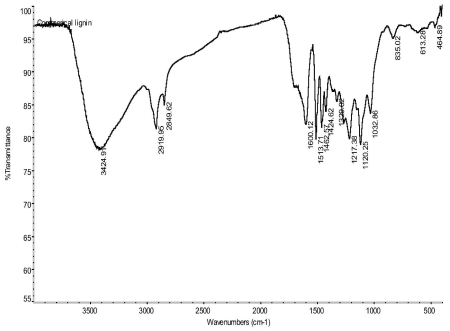

Figure 28. FT-IR Spectrum of Commercial Lignin

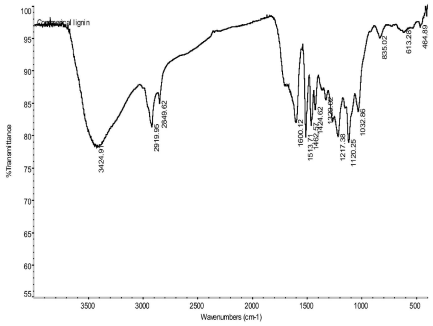

Figure 29. FT-IR Spectrum of untreated bagasse lignin

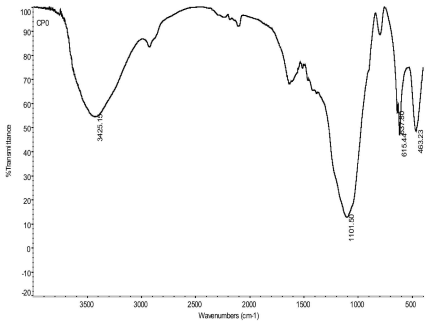

Figure 30. FT-IR Spectrum Bagasse Lignin – zeroth week (Control sample)

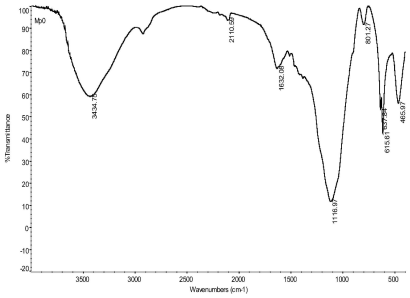

Figure 31. FT-IR Spectrum of Treated Lignin – zeroth Week

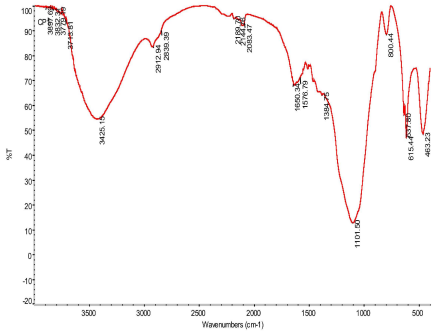

Figure 32. FT-IR Spectrum of Treated Lignin – Week 1 (Control sample)

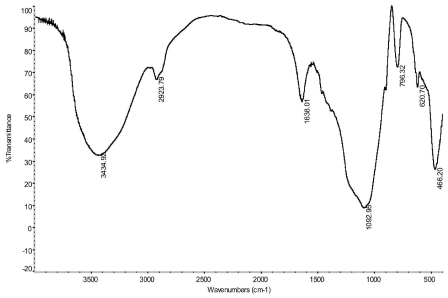

Figure 33. FT-IR Spectrum of Treated Lignin – Week 1

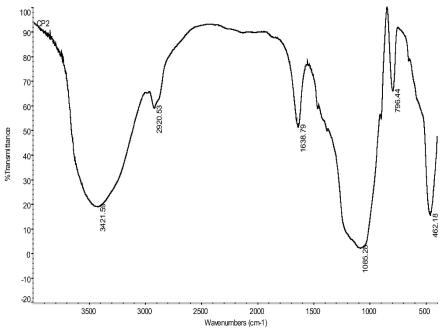

Figure 34. FT-IR Spectrum of Treated Lignin – Week 2 (Control sample)

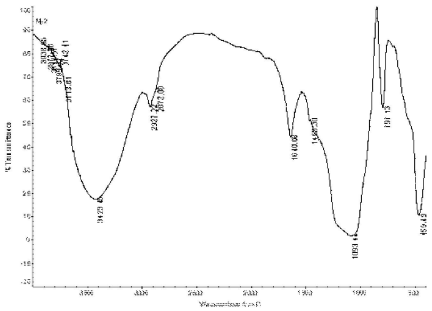

Figure 35. FT-IR Spectrum of Treated Lignin – Week 2

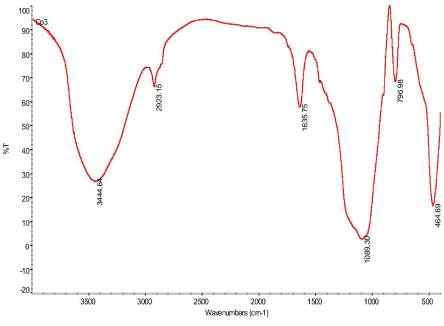

Figure 36. FT-IR Spectrum of Treated Lignin – Week 3 (Control sample)

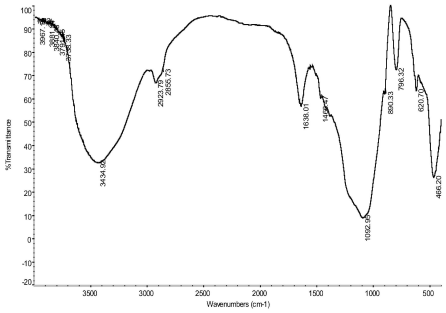

Figure 37. FT-IR Spectrum of Treated Lignin – Week 3

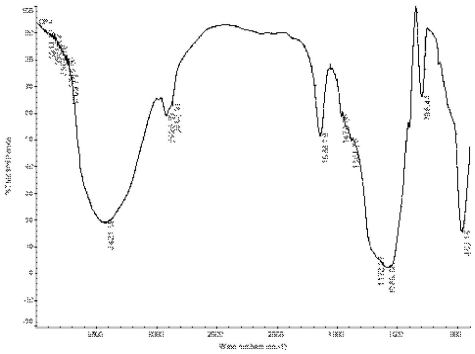

Figure 38. FT-IR Spectrum of Treated Lignin – Week 4 (Control sample)

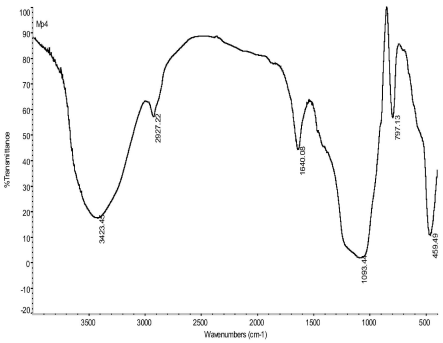

Figure 39. FT-IR Spectrum of Treated Lignin – Week 4

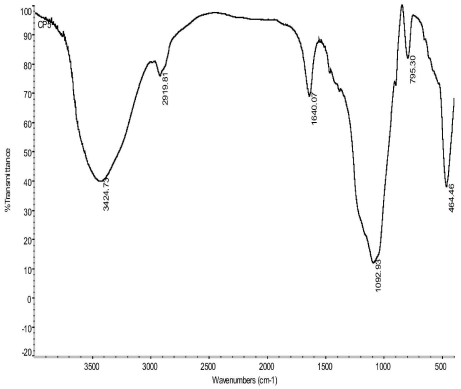

Figure 40. FT-IR Spectrum of Treated Lignin – Week 5 (Control sample)

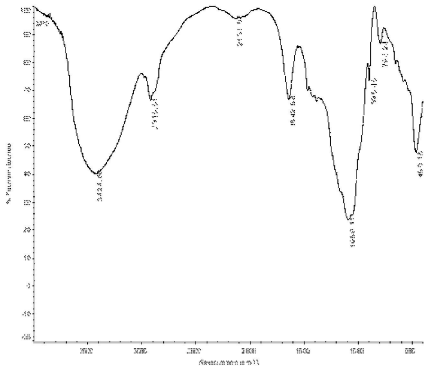

Figure 41. FT-IR Spectrum of Treated Lignin – Week 5

The FTIR spectrum of commercial lignin shows the characteristic peaks corresponding to phenolic O–H, aliphatic C–H, aromatic skeletal vibrations, and C–O stretching. The spectrum confirms that the sample is indeed lignin, with distinct absorption bands characteristic of its complex polymeric structure. The overall complexity of the spectrum, with many overlapping peaks in the fingerprint region, is typical of a natural, complex polymer like commercial lignin (Figure 28-29). This spectrum of untreated bagasse in the control sample from the zeroth week is characteristic of raw lignocellulosic material with a high mineral content, such as bagasse. These peaks are broad, which is common for complex composite materials—attributed to bending of Si-O groups—further confirming the high mineral/silica content in the raw material (Figure 30-32). Infrared spectrum of lignin extracted after one week of fungal treatment, showing initial reductions in O–H and aromatic C=C stretching bands, indicating early-stage oxidative modification

(figure 33-34). Spectrum showing progressive decreases in aromatic skeletal vibrations and ether linkage peaks compared to untreated lignin, reflecting increased depolymerization during the second week (Figure 35-38). FT-IR spectrum showing significant reductions in aromatic ring absorbance and the emergence of weak carbonyl peaks, indicating active enzymatic oxidation and cleavage of lignin units (Figure 37). Spectrum in figure 39 showing pronounced structural alteration, including diminished O–H, C–O, and aromatic peaks, with clear evidence of formation of oxidized functional groups (e.g., C=O at ~1720 cm^{-1}). Final stage FT-IR spectrum of biosoftened lignin, exhibiting the most substantial reduction in aromatic peaks and maximal presence of carbonyl-associated absorbances, confirming extensive lignin degradation by *Pleurotus sajor-caju* (Figure 40-41). Overlay of weekly FT-IR spectra illustrating the progressive loss of aromatic and phenolic structures and the emergence of oxidation products across the treatment period. This visual comparison highlights the cumulative impact of fungal lignin-olytic activity.

The results of UV scanning and FTIR indicate structural differences between the commercial lignin, treated lignin, and control samples. This is due to the fungus Pleurotus sajor caju degrading lignin during solid-substrate fermentation.

5. Conclusion

Through solid-substrate fermentation, the study effectively demonstrated the efficiency of Pleurotus sajor-caju in degrading lignin in bagasse. The key to softening lignin molecules was the production of lignin-degrading enzymes by Pleurotus sajor-caju, including manganese peroxidase, lignin peroxidase, and cellobiose dehydrogenase. When the extracted lignin was compared with synthetic lignin, UV and FT-IR analyses revealed notable structural alterations, suggesting lignin softening. These results imply that Pleurotus sajor-caju's enzymatic activity enhances lignin's binding efficacy, making it a feasible biological approach for the production of lignin-phenol-formaldehyde resins. This work emphasizes how the bioconversion of agricultural leftovers by white-rot fungi might lead to more sustainable and effective industrial processes.

The combined evidence from yield data, UV spectroscopy, and FT-IR analysis demonstrates the efficacy of *Pleurotus sajor-caju* in biosoftening lignin. The substantial decrease in lignin yield, accompanied by spectral changes, highlights the enzymatic role of this white-rot fungus in lignin degradation.

The results suggest that solid-substrate fermentation with P. sajor-caju can be an eco-friendly, cost-effective method for lignin modification, thereby reducing reliance on harsh chemical treatments. This aligns with previous reports that white-rot fungi are promising biocatalysts for valorizing lignocellulosic residues.

The modified lignin obtained from this process shows potential for use in resin synthesis, particularly lignin–phenol–formaldehyde resins, which require softened lignin for effective crosslinking. Thus, this study not only demonstrates the biodegradability of *P. sajor-caju* but also its industrial applicability for sustainable polymer production.

References

[1] Asada, C., Basnet, S., Otsuka, M., Sasaki, C., Nakamura, Y. (2015). Epoxy resin synthesis using low molecular weight lignin separated from various lignocellulosic materials. *Int J Biol Macromol* 74, 413–419.

[2] Barreira, J. C. M., Oliveira, M. B. P. P., Ferreira, I. C. F. R. (2014). Development of a novel methodology for the analysis of ergosterol in mushrooms. *Food Anal. Methods* 7, 217–223.

[3] Caglarirmak, N. (2007). The nutrients of exotic mushrooms (Lentinula edodes and Pleurotus species) and an estimated approach to the volatile compounds. *Food Chem*. 105: 1188–1194.

[4] Kurt, S., Buyukalaca, S. (2010). Yield Performances changes in enzyme activities of Pleurotus spp. (P. ostreatus and P. sajor-caju) cultivated on different agricultural wastes. Biores. *Technol.*, 101, 3164-3169.

[5] Mane, V. P., Patil, S. S., Syed, A. A., Baig, M. M. V. (2007). Bioconversion of low quality lignocellulosic agricultural waste in to edible protein by Pleurotus sajor-caju (Fr.) Singer. J. Zhejiang Univ. *Sci. B.,* 8, 745-751.

[6] Huo, Meiyu., Chen, Jian., Jin, Can., Huo, Shuping., Liu, Guifeng., Kong., Zhenwu (2024). Preparation, characterization, and application of waterborne lignin based epoxy resin as eco-friendly wood adhesive, *International Journal of Biological Macro mole cules,* Volume 259, Part 2.

[7] Nelliyat, P. (2003). Coconut husk retting and backwater pollution in coastal Kerala. 3rd biennial conference of the Indian Society for Ecological Economics*, Kolkata*.

[8] Shashirekha, M. N., Rajaratham, S., Bano, V. (2002). Enhancement of biocon version efficiency and chemistry of the mushroom, Pleurotus sajor-caju (Berk and Br.) Sacc. Produced on spent rice straw substrate, supplemented with oil seed cakes," *Food Chemistry,* vol. 76, p. 27-31.

[9] Oei, P. (2003). Mushroom cultivation. Appropriate Technology for mushroom grawres. (3 rd ed). *Leiden, Netherlands: Backhuys Publisher*.

[10] Reis, F. S., Martins, A., Barros, L., Ferreira, I. C. F. R. (2012). Antioxidant properties and phenolic profile of the most widely appreciated cultivated mushrooms: A comparative study between in vivo and in vitro samples. *Food Chem. Toxicol.* 50, 1201–1207.

[11] Yogitha, B., Karthikeyan, M., Muni Reddy, M. G. Progress of sugarcane bagasse ash applications in production of Eco-Friendly concrete Review, Materials Today: Proceedings, https://doi.org/10.1016/j.matpr.2020.05.814.

[12] Rosli, Wan., W. I., Nurhanan, A. R., Aishah, M. S. (2012). Effect of partial replacement of wheat flour with oyster mushroom (Pleurotus sajor-caju) powder on nutritional composition and sensory properties of butter biscuit. *Sains Malaysiana* 41 (12), 1565-1570.

[13] Wasser, S. P. (2002). Medicinal mushrooms as a source of antitumor and immunomodulating polysaccharides. *Applied Microbiology and Biotechnology* 60, 258-274.

[14] Wongsangprai, C. (2012). Bag Cultivation of Mushroom, Kasetsiam, Bangkok, , ch. 1, p. 7-9.

[15] Chahal, D. S., Hachey, J. M. (1990). Agricultural and Synthetic Polymers Vol. 443, Chapter 25 p 304-310. *American Chemical Society*.

[16] Mpadi, N. C., Bangala, D.-B.). M. (2020*)* Utilisation du champignon Pleurotus sajor-caju pour la délignification d'un substrat à base des hampes florales de bananiers (Musa spp.) et la production des carpophores comestibles. *International Journal of Biological and Chemical Sciences,* 13 (7), 3164–3176. https://doi.org/10.4314/ijbcs.v13i7.16).

[17] Helena, Sá., Michelin, Michele., Silvério, Sara., C. Lourdes, Maria de., T. M., Polizeli, Silva, Ana., R., Pereira, Luciana., Tavares,Teresa., Silva, Bruna . (2024). Pleurotus ostreatus and Lentinus sajor-caju laccases for sulfamethoxazole biotransformation: Enzymatic degradation, toxicity and cost analysis, *Journal of Water Process Engineering,* Volume 59, 2024, 104943.

[18] Ji, C. J., Hou, K., Wang, Y., Zhang, V., Chen. (2016). Biocatalytic degradation of carbamazepine with immobilised laccase-mediator membrane hybrid reactor, J. Memb. Sci., 502 (2016), p. 11-20.